LA-UR- 08-5476

Approved for public release; distribution is unlimited.

Title:	Performance evaluation of booster materials in the plastic bonded explosive PBX 9502 in a hemispherical wave breakout test
Author(s):	Daniel E. Hooks, John S. Morris, Larry G. Hill, Elizabeth Francois, Herbert H. Harry
Intended for:	revised submission to Propellants, Explosives, & Pyrotechnics

Los Alamos
NATIONAL LABORATORY
EST. 1943

Form 836 (7/06)

Performance evaluation of booster materials in the plastic bonded explosive PBX 9502 in a hemispherical wave breakout test

Daniel E. Hooks*, John S. Morris, Larry G. Hill, Elizabeth Francois, Herbert H. Harry

Los Alamos National Laboratory

P.O. Box 1663, Los Alamos, NM 87544 US

(Received: June 12, 2008)

DOI: 10.1002/prep.200700000

Abstract

An explosive booster is normally required to initiate detonation in an insensitive high explosive (IHE). Booster materials must be ignitable by a conventional detonator and deliver sufficient energy and favorable pulse shape to initiate the IHE charge. The explosive booster should be as insensitive as reasonably possible to maintain the overall safety margin of the explosive assembly. A hemispherical wave breakout test termed the onionskin test is one of the methods of testing the performance of booster materials in an initiation train assembly. There are several variations of this basic test which are known by other names. In this test, the wave breakout time-position history at the surface of a hemispherical IHE acceptor charge is recorded, and the relative uniformity of breakout allows qualitative comparison between booster candidates and quantitative comparison of several metrics. The results of a series of onionskin experiments evaluating the performance of some new booster formulations in the triaminotrinitrobenzene (TATB) - based plastic bonded explosive PBX 9502 will be presented. The boosters were tested in an onionskin arrangement in which the booster pellet was cylindrical, and the tests were performed at a temperature of -55°C to emphasize variations in spreading performance. The modification from the traditional hemispherical geometry facilitated efficient explosive fabrication and charge assembly, but the results indicate that this geometry was not ideal for several reasons. Despite the complications arising from geometry, promising performance was observed from booster formulations including 3,3'-diamino-4,4'azoxyfurazan.

Keywords: explosive booster performance, detonation wave reconstruction, diaminoazoxyfurazan, onionskin test

1 Introduction

Initiation of detonation in insensitive high explosive formulations normally requires the use of a booster explosive in the initiation train. The choice of the booster material is crucial as

* Corresponding author; e-mail: dhooks@lanl.gov

the initiation train must function reliably across some spectrum of physical parameters and the safety margin of the assembly is enhanced by the insensitivity of the booster. The booster must be sufficiently sensitive to initiate detonation and spread efficiently through the charge. Other important properties include the density, shock impedance, and thermal expansion coefficient, to name a few. Finally, the safety properties of the booster explosive must ensure the required margins for the explosive assembly as a whole.

A number of materials have been used as boosters in the past. The focus of this paper is to present a series of booster tests with a booster geometry designed for expedient manufacture and assembly of explosive parts. Booster material performance is evaluated in the triaminotrinitrobenzene (TATB) - based plastic bonded explosive PBX 9502 acceptor explosive. This formulation is composed of 95% TATB and 5 % fluorinated copolymer (3M Kel-F 800).

Booster test experiments have been performed in many ways. In several of these tests, a booster material is inserted in a hemispherical shell of main charge explosive, and this subassembly is initiated with a conventional detonator. The wave breakout from the hemisphere is observed with a streak camera and from this time-position record the wave shape in the material and the "center of initiation" can be inferred. Initiation of the train has been achieved with a detonator directly under the booster in a direct contact or flyer configuration, or with another charge in a cylindrical configuration beneath the booster. Similar variations of this basic test have been known as "half-peach," "snowball,"[1] and "onionskin."[2], [3] The "mushroom"[4] test is closely related, but is designed to observe breakout from the booster directly, which is ignited by a stem of well-characterized conventional high explosive. In most test designs, the booster geometry is also hemispherical, so that the emergent wave is nominally spherical. The spherical wave, although never strictly achieved, allows a simple wavefront reconstruction, wherein a circular fit to the wavefront can allow determination of the center of initiation (COI) in the assembly. It is noted that in any case other than a perfectly spherical wave, there is never a "true" center of initiation, but rather a "zone of confusion" by analogy to optical analysis.[5]

In the experiments described, several new booster formulations were evaluated in an onionskin test performed at low temperatures to evaluate the spreading characteristics of the booster materials. While the remainder of this paper will focus on the onionskin test in particular, the results are relevant to tests of similar design. The main modification made in the current tests was the replacement of the hemispherical booster pellet with one in a cylindrical configuration. This change enabled more efficient and inexpensive part fabrication and assembly, but forced a change from a previously developed analysis approach.[6]

2 Experimental

The experimental assembly is shown schematically in Figure 1. An ER 400 detonator used in an flyer configuration was mated to a booster pellet that was 10 mm thick and 30mm in diameter. The detonator was set at a standoff distance of 1.651 mm from the booster pellet, and its 0.165 mm thick aluminum flyer was sheared by the fixture to a diameter of 5.766 mm. The velocity of

the flyer at impact with the booster pellet was 3.75 ± 0.25 km/s. The booster pellet was mounted in a 50 mm outer diameter hemisphere of PBX 9502. This assembly was mounted on a fixture machined from cast aluminum (MIC-6 tooling plate) for dimensional stability as temperature is decreased. The fixture incorporates a pair of mirrors for observation of breakout from the sides of the PBX 9502 hemisphere, and a fiducial detonator on the same plane as that under the charge assembly. The dimensional stability of the fixture is crucial, allowing facile combination of direct and indirect streak records of the breakout. The surface of the fiducial detonator flyer and the PBX 9502 charge was painted with an aluminum fluorosilicate phosphorescent salt to both increase and make uniform the emitted light from the breakout event.

<figr1>

The assembly was cooled to -55°C in an insulated chamber prior to firing by flowing nitrogen gas over liquid nitrogen with an inline heater for control. Ramp rates were controlled at 0.5°C/min. The temperature of the gas inlet and of four locations on the charge assembly was monitored and recorded, and the assembly was soaked at the final temperature for a minimum of 30 min. The low temperature of firing emphasizes variations in spreading performance and wave perturbations. The breakout from the fiducial detonator and the surface of the main charge was recorded on a Cordin model 132 streak camera operating at a write speed of 12 mm/μs. A still image of the experiment was taken on the same film prior to firing. The experiments were fired in an enclosed firing vessel.

Booster formulations evaluated are listed in Table 1. The ultrafine TATB (UF-TATB), LX-07, and PBX 9504 formulations have been tested in the past. LX-07 is a plastic bonded explosive developed by Lawrence Livermore National Laboratory consisting of cyclotetramethylene tetranitramine (HMX) and DuPont Elastomers Viton A. PBX 9504 is a plastic bonded explosive developed by Los Alamos National Laboratory consisting of TATB, pentaerythritol tetranitrate (PETN), and 3M Kel-F 800, and was formerly the experimental formulation designated X-0407. The LX-07 formulations were selected as nominal standards for this test. 3,3'-diamino-4,4'-azoxyfurazan (DAAF) and 3,6-diamino-s-tetrazine-1,4-dioxide (LAX-112) are experimental formulations. Molecular structures for DAAF and LAX-112 are shown in Figure 2.

<figr2>

The DAAF used in this experiment was from a new recrystallization method. The traditional synthesis of DAAF creates an impure product which requires purification.[7] Typically, the synthesis product is purified by crash precipitation from dimethyl sulfoxide (DMSO) and water. Small particle sizes (~5μm) resulting from the DMSO purification inhibit pressing to high density. Preliminary performance tests exhibited poor performance as a result of the low pressed density. To grow larger crystals, the DAAF was recrystallized in acetonitrile (ACN). Larger particle sizes from this process (~20μm) enabled the DAAF pellets to be pressed to a density of 1.693 g/cc which is 97% theoretical maximum density (TMD) as opposed to previous efforts where the highest achievable density was 1.60 g/cc (91% TMD).[7, 8]

LAX-112 synthesis and recrystallization is time-consuming and expensive, and for efficiency reclaimed material was used. The formulation was performed by both slurry and hand mixing. Tests have indicated performance enhancements with the hand mixing method.

A Carver 20-ton hydraulic press was used to press the booster pellets. Each booster required a different method to press, as highest possible density was the goal. Generally, the HE was heated to 85°C and pressed in a die heated to the same temperature in a press with heated platens. Intensification was used to improve the density, with two 5-minute dwell cycles separated by a 1-minute relaxation. The force applied was material dependent. The PBX 9504 was pressed cold as it tended to crack horizontally when heated and then extracted from die. A dimpling effect was noted on the LX-07 pellets, where the surface of the pellet appeared to be delaminating in the top-center.

The density of the pellets was calculated from dimensions and mass. Immersion density could not be performed on neat-pressed DAAF as it tends to absorb the immersion media. For consistency, the density of all pellets is presented using the dimensional method. Because of limited availability of these materials, the pressed-to-shape approach of using a cylindrical booster was a significant advantage.

PBX 9502 parts were machined from a billet pressed to a density of 1.890 +/- 0.005 g/cc. The PBX 9502 lot was HOL88H891-008. The booster pellets were mated to the PBX 9502 charges using Aralhex glue. Some booster pellets varied from perfect co-planarity by as much as 0.5 mm over the 30mm width. In these cases, the flat side was mated into the PBX 9502 and the charge was oriented on the fixture such that the tilt axis was perpendicular to the camera slit.

<tabr1>

3 Results

A representative photo showing the still frame and streak record for one of the experiments has been shown previously.[9] Cooling profiles (not shown) were recorded on a personal computer and stored. Scanned films for all of the successful experiments are shown in Figure 3. Note inflections in the PBX 9504 and DAAF records. The LX-07 records were relatively smooth in their breakout behavior by comparison. The fiducial detonator record was unreadable on the film for the Dyed LX-07 experiment. The analysis for this experiment matched the timing of first breakout for the other LX-07 experiment. Both of the LAX-112 formulations failed to initiate in this configuration. In the case of the LAX-112 / Kel-F 800 formulation, there was no unreacted explosive found in the firing vessel after the experiment, but the relative amount of damage observed was significantly decreased from the typical amount and no streak record was obtained. Unreacted pieces of the LAX-112 / Viton A formulation and the PBX 9502 main charge, some still glued together, were found intact in the vessel after firing. The UF-TATB formulation showed hole-punching behavior, wherein detonation proceeded from the detonator, but did not spread through the charge. Unreacted PBX 9502 was found in the vessel in a circular line around the experiment after firing.

<figr3>

4 Analysis

High quality scanned film was digitized directly with an image processing application. This digitization was compared with the results from an optical comparator and the differences were negligible. Automated edge recognition was not employed; the edge recognition was performed manually to avoid complications with "dropout" events that were observed, presumably due to non-uniformities in the phosphorescent paint. Following digitization, the mirror records were combined with the direct records using the still image as a guide for position. The digitized and combined records are shown for all successful experiments in Figure 4.

<figr4>

The change to a cylindrical booster pellet in the hemispherical test induced a complication in analysis. The deviation from a spherically symmetric wave was severe in all cases, even in the case suspected to be closest to ideal: that of the LX-07 booster. Since a spherical (or nearly spherical) wave is an important assumption to the previously developed analysis of these tests,[6] another approach was required. The previous analysis had developed to a point of relying on the COI metric with a fixed interval of fit, disregarding the comparative results of the wave reconstruction. The current results required a qualitative judgment about the wave reconstruction, and the window of fit for the COI had to be adjusted for each to avoid an infinite result from the "flat" wave shapes observed.

The first breakout angle (FBA) was deduced directly from the records. In a cross-sectional view of the hemispherical charge, a vertical line bisecting the hemisphere crosses the edge of the charge at zero degrees, and the flanks are at plus or minus 90 degrees. The FBA is the angular position on the PBX 9502 hemisphere measured from zero degrees where first light is detected, and as such is the primary metric of spreading. The "spreading efficiency" was defined as FBA/90.

Assuming that the detonation travels at a constant speed D normal to itself, one can deduce the shape of the detonation shock from the breakout time versus angle plot.[10] Subject to this one assumption, this wavefront construction is valid for any time after initiation—either before, during, or after the detonation breaks out of the ball. Wavefronts corresponding to regions outside of the ball provide an estimate of how the wave would have propagated if the HE continued past the actual observation surface.

In practice, obvious pathologies develop if the wavefront is propagated very far backward in time. The origin of the problem is that real detonations do not travel at a constant velocity; rather, their local normal speed depends on the local curvature. The curvature dependence is modest for conventional explosives like PBX 9501, but is substantial for non-ideal explosives like PBX 9502.

Curvature effects are accurately and efficiently computed by the detonation shock dynamics (DSD) model, which, in its most basic form, assumes that the normal detonation speed D_n is a function of the curvature κ (e.g., [11]). J. Bdzil has shown that wavefront reconstruction (a type of inverse problem) is ill posed for the DSD prescription.[13] Although these real non-ideal material effects cause a degree of error, the constant speed approximation is nevertheless good enough to be extremely useful.

The average detonation speed through the ball is given by its radius R, divided by the transit time t_t of the detonation along the axis. Referring to the film record, t_t is the detonation breakout time on the ball axis, less the detonation breakout time on the fiducial detonator face. The speed R/t_t is not an ideal number to use for D, because 1) the wave is the process of initiating, and 2) the booster is a different explosive with a different detonation speed. In practice, it is generally better to use D-values obtained from other experiments. The assumed value of 7.6 mm/μs used in this study is typical of that measured in a 1-inch diameter PBX 9502 copper cylinder test.

The detonation wave shape curls back, such that its contour is a multi-valued function in Cartesian coordinates. This requires the curve to be represented parametrically as a function of the angle θ measured from the pole. The wave shape will also depend on the ball radius R, and detonation speed D, and the evaluation time t. Consequently, we seek a description of the form:

$$x = \mathrm{fn}_1[\theta, t, R, D], \quad y = \mathrm{fn}_2[\theta, t, R, D]. \tag{1}$$

Figure 5 shows the construction geometry. A small portion of the wave is shown emerging from the ball at an angular position θ. The wave emerges at an angle α with respect to the observation surface. If the emerging wave conformed exactly to the observation surface, its shape as it emerged would be:

$$x = R\sin[\theta], \quad y = R\cos[\theta]. \tag{2}$$

<figr5>

In real problems for which this is not the case, one may express the wave shape in terms of a deviation from this reference case. The diagram of Figure 5 shows that if the evaluation time t is different than the breakout time τ, then the wavefront position is displaced a distance $D(t - \tau)$, in the direction of propagation of the wavefront at that location. Adding this correction yields:

$$x = R\sin[\theta] + D(t-\tau)\sin[\theta+\alpha], \qquad y = R\cos[\theta] + D(t-\tau)\cos[\theta+\alpha]. \tag{3}$$

A condition $t > \tau$ puts the wave outside the ball; a condition $t < \tau$ puts the wave inside the ball. If $\alpha = 0$, then the wavefronts are circles centered at the geometric ball center, for which the condition $t = \tau$ conforms to the observation surface (thus recovering Eq. 2).

The ball radius R is accurately measured prior to the shot. The most appropriate value of the detonation speed D is estimated from other experiments. The breakout time τ is measured by the streak camera as a function of θ:

$$\tau = f[\theta] \tag{4}$$

Thus, the only unknown in variable in Eqs. 3 is the angle α. Figure 6 shows the geometric construction by which α can be related to known quantities.

<figr6>

The detonation breakout front travels along the observation surface at a phase speed $\dot{s}$. From Figure 6, it is clear that:

$$\sin[\alpha] = \frac{D}{\dot{s}}. \tag{5}$$

Moreover,

$$\dot{s} = \frac{\mathrm{d}s}{\mathrm{d}t} = R\frac{\mathrm{d}\theta}{\mathrm{d}t} = \frac{R}{\mathrm{d}t/\mathrm{d}\theta} = \frac{R}{\mathrm{f}'[\theta]}. \tag{6}$$

where $\mathrm{f}'[\theta]$ is the derivative of Eq. 4. Substituting Eq. 6 into Eq. 5 and solving for α gives:

$$\alpha = \arcsin\left\lfloor \frac{D\mathrm{f}'[\theta]}{R} \right\rfloor. \tag{7}$$

Because differentiating data introduces noise, it is necessary to smooth the function $\mathrm{f}[\theta]$ in order to obtain a sufficiently smooth function $\mathrm{f}'[\theta]$. On the other hand, too much smoothing will erode real features of the wavefront, such as how the wavefront is affected by the corner of the cylindrical booster. A smoothing routine developed by T. Salyer [13] that balances these requirements was used. It is based on the idea that an ideal fit is one that produces a structure-less ("white noise") residual pattern. The smoothing routine removes unwanted noise while maintaining the underlying real structure.

Finally, it should be noted that the entire reconstruction scheme relies on an important property of waves that travel at a constant speed, such as an ideal detonation or a light wave. Choose any point on the wave and draw a normal line through it. The wave propagates forward in such a way that the wave always remains normal to that line. Likewise, the wave motion prior to that point (retraced by propagating the wave backward in time) was also normal to that line. It is this feature that allows one to unambiguously translate the wave, as it breaks out of the ball, forward or backward in time.

Using this technique, two wave reconstructions were performed for each experiment. In the first, all points of the wave were "pushed back" into the hemisphere from the point at the FBA. In the second, all points of the wave were "pulled forward" out of the hemisphere from the point at the last breakout angle. These two wave reconstructions are shown for each of the experiments in Figure 7, along with the wave constructed by averaging the two approaches.

<figr7>

The COI was determined by taking an average of the two reconstructed waves (shown in Figure 5) and fitting a circle to the region bounded by the FBA. The excess transit time, or the increased transit time as compared with the time required for a detonation to traverse the 50mm hemisphere if it were all detonating PBX 9502, is the final metric defined here to compare results. These times are comparatively longer than would be deduced based on detonating material because the booster must first progress through a shock to detonation transition which can be somewhat lengthy at low temperature. A summary of all of the results is given in Table 2.

<tabr2>

5 Discussion

The wave reconstruction method described here has limitations, but the analysis allows a facile method for qualitative comparison between records. Simply propagating waves in a Huygens construction exaggerates any perturbations. The reconstruction shown in Figure 7 that was pulled forward from last observed breakout exhibits this anomaly quite clearly at angles near 90 degrees. It is for this reason that the COI analysis was performed on the average of the 2 wave reconstructions. It would be better to iteratively run a detonation shock dynamics code, which accounts for detonation speed variation with curvature, material geometry, and edge interactions properly, until a match to experimental observations is obtained. Additionally, breakout data directly from the booster materials would be very helpful. Modeling and booster experiments are left to future work.

Given that there is no "true" COI in any similar experiment, the COI presented always depends sensitively on the range of angles used in the circular fit to find it. The numbers presented here would obviously change significantly if the range of the fit were expanded or contracted. An important conclusion is that the approach to finding COI should be carefully considered for each experiment individually and comparisons between non-identical experimental configurations is perilous.

The LX-07 formulation was expected to perform very well and did as measured by the COI, FBA, and wave shape. There is little evidence in the wave reconstructions that the booster was cylindrical other than a somewhat flat wave reconstruction profile. The addition of dye to the formulation made no difference in the results, which is important given the changing availability of ingredients to make new lots of material with older formulation procedures. While the LX-07 performed well, it is purely HMX based, and the hope was to find a newer material with somewhat decreased sensitivity properties.

UF-TATB was considered highly likely to fail in this configuration at this temperature. UF-TATB can perform admirably even at low temperatures, but requires longer run distances. In the geometry tested here, the booster was undersized to a significant disadvantage in this regard. In fact, the observed behavior of hole punching, while a failure for the charge assembly performance, is quite interesting as a case of understanding the stability of detonation in TATB and its formulations and calibrating models designed to predict their performance. The current test revealed a detonation just on the margins of stability. Slight changes to booster size and/or temperature would likely change the system to divergent detonation or extinction.

In unpublished experiments at ambient temperatures, formulations based on LAX-112 had performed well. However, the run distance as a function of input pressure is somewhat long, and lacking data at cold temperatures its performance was not certain. In fact, both formulations failed to ignite in the current experiments. It is not known at this time if larger booster sizes or a detonator with different pulse shape might be effective in igniting these materials at low temperature.

PBX 9504 has been tested previously at a variety of temperatures in the hemispherical onionskin test. Given its previous success, it was expected to perform admirably. The PBX 9504 formulation must be performed properly to ensure material uniformity, but is not an issue if carefully controlled. It has not been tested previously in cylindrical geometry, however. The current results reveal what might have been the best results of all in terms of approaching spherical wave shape if not for inflections at the flanks of the hemisphere. Although the inflections seem to originate at the corners, the origin of these features is hard to pin-point. The density of the PBX 9504 is very close to PBX 9502. Detonation velocity differences might result in wave reflections at the interface, but these differences would be expected just as clearly in the LX-07 tests and were not observed. Thus the inflections are not understood, but might be due to material uniformity or detonation velocity differences. A detonation shock dynamics simulation of the system might elucidate the reasons. If the detonation velocity is the culprit, then a booster in a hemispherical configuration should alleviate the problem.

DAAF exhibited large perturbations in wave shape, most likely caused by wave reflections at the corners of the cylinder from impedance differences arising from an appreciably lower pressed density than PBX 9502. Given the history of impurity and particle quality issues in this material,[7, 8] such features might also be explained by uniformity gradients in the material, but this seems far less likely. However, the spreading efficiency of DAAF was the best of all of the boosters tested, and the COI was comparable to LX-07. Efficient and reduced-waste processes have been discovered for synthesis and recrystallization of DAAF (unpublished, patent pending). Given the success in performance metrics, the overall net improvement in safety that DAAF might promise, and the favorable processes for manufacturing DAAF, future experiments are planned on differently processed DAAF in different booster geometries to investigate the source of the wave perturbations.

Future experiments will focus on the processing parameters and geometry of DAAF and PBX 9504. Both of these materials were very promising by the metrics of COI and FBA, but clearly need further evaluation. Impedance differences might be improved for DAAF by formulation with high density polymers, but it is doubtful that they could be completely eliminated for because of the low TMD of DAAF itself. However, impedance differences may be less important in the hemispherical booster geometry because wave reflections would be less important, and the resulting analysis is much more ideal, so experiments in this configuration will be performed in parallel.

6 Conclusions

In summary, the LX-07 booster performed well, as expected, and the addition of dye to the formulation made no observable difference. The DAAF showed very promising results in terms of detonation spreading, but exhibited perturbed waves indicative of either material uniformity problems or detonation wave reflections at the corners of the booster pellet due to density mismatch with the PBX 9502. The PBX 9504 wave exhibited some small perturbations, but not nearly so severe, and otherwise performed well. The UF-TATB exhibited hole-punching behavior, in which the center of the charge ignited but the detonation did not spread. This was to be expected, a UF-TATB booster at this temperature should be roughly 5 times larger to allow the required run distance. Finally, both of the formulations including the LAX-112 molecule completely failed to ignite in the tested configuration, and therefore no data was obtained.

The simple change in experimental design from a hemispherical to a cylindrical booster had serious consequences. While the manufacture and assembly of parts was simplified, the analysis approach was complicated. Wave interactions due to shock impedance mismatches were of increased importance and the overall wave shape required a change in the approach for determining COI.

The PBX 9504 and DAAF results were quite promising. Spreading performance and initiation of the PBX 9502 proved reliable even at the low temperature at which the tests were performed. However, the wave shape perturbations are of concern and merit more study. PBX 9504 has been known to be a challenge in formulation; the disparate solubility of PETN and TATB can cause uniformity issues in formulation and pressing. Purity, particle quality, and uniformity issues have been noted in DAAF as well.[7, 8] In fact, a new synthetic route and recrystallization procedure have been developed to improve these features. While these uniformity issues could be problematic, it is more likely that the perturbations were caused simply by wave reflections due to impedance differences. Impedance differences may not matter as much if the geometry of the booster matches that of the desired wave spreading geometry. For this reason, future experiments will focus on formulation and pressing changes in PBX 9504 and DAAF in a hemispherical geometry. Furthermore, DSD modeling and breakout experiments on the boosters themselves would be very helpful in understanding these results.

7 References

[1] A. W. Lundberg, High Explosives in Stockpile Surveillance Indicate Constancy, *Science & Technology Review*, Lawrence Livermore National Laboratory, Livermore, CA, USA, **1996**, UCRL-52000-96-12, p. 12.

[2] J. C. Dallman, *Measurements of Detonation-Wave Spreading and Local Particle Velocity at the Surface of 17-mm LX-07 Hemispherical Boosters*, Report LA-11414-MS, **1988**, Los Alamos National Laboratory, Los Alamos, NM, USA.

[3] G. E. Hogan et al, Proton Radiography, in A. Luccio, W. MacKay (Eds.), *Proceedings of the 1999 Particle Accelerator Conference, Vol. 1*, IEEE, Piscataway, NJ, **1999**, p. 579.

[4] L. G. Hill, W. L. Seitz, C. A. Forest, H. H. Harry, High Explosive Corner Turning Performance and the LANL Mushroom Test, in S. C. Schmidt, D. P. Dandekar, J. W. Forbes (Eds.), *Shock Compression of Condensed Matter - 1997*, AIP Conference Proceedings, Woodbury, NY, **1997**, p. 751.

[5] M. Busco, Optical Properties of Detonation Waves (Optics of Explosives), *Fifth Symposium (International) on Detonation*, Office of Naval Research, Arlington, VA, **1970**, p. 513.

[6] E. S. Martin, H. L. Mallett, Apparent Center of Initiation Analysis for Explosive Investigations, *37th International Annual Conference of the ICT*, Fraunhofer Institut fur Chemishe Technologie, Karlsruhe, Germany, **2006**, p. 108.

[7] D. E. Chavez, L. G. Hill, M. A. Hiskey, S. A. Kinkead, Preparation and Properties of Azo- and Azoxy- Furazans, *Journal of Energetic Materials*, **2000**, *18*, 299.

[8] M. A. Hiskey, D. E. Chavez, R. L. Bishop, J. F. Kramer, S. A. Kinkead, *Use of 3,3'-diamino-4,4'-azoxyfurazan and 3,3'-diamino-4,4'-azofurazan as Insensitive High Explosive Materials*, U. S. Patent 6358399 **2002**, Los Alamos National Laboratory, USA.

[9] D. E. Hooks, J. S. Morris, L. G. Hill, E. G. Francois, H. H. Harry, Performance Evaluation of Booster Materials with a Modified Onionskin Test, *39th International Annual Conference of ICT*, Fraunhofer Institut fur Chemische Technologie, Karlsruhe, Germany, **2008**.

[10] The wavefront reconstruction process described in this paper is based on the analysis of Charles Forest, at LANL, in the early 1990's. Despite widespread internal use, that analysis has not been published.
[11] T. D. Aslam, J. B. Bdzil, D. S. Stewart, Level Set Methods Applied to Modeling Detonation Shock Dynamics, *Journal of Computational Physics*, **1996**, *126(2)*, 390.
[12] J. B. Bdzil, *Inverse Problems in Detonation Front Evolution*, Los Alamos National Laboratory Internal Memorandum to Charles Forest, #M7:92-0375, **1992**.
[13] T. R. Salyer, private communication, **2008**.

Acknowledgments

We are grateful to Bart Olinger for performing explosive assembly and to Larry Vaughan and Bob Mier for assisting in setup and firing of the experiments. This work was funded by the National Nuclear Security Administration Science Campaign 5, under the direction of Rob Bishop and David Montoya. LA-UR-08-xxxxx.

Symbols and Abbreviations

FBA	first breakout angle
ACN	acetonitrile
DMSO	dimethylsulfoxide
COI	center of initiation
PBX	Plastic bonded explosive
LAX	Los Alamos explosive
LX	Livermore explosive
HMX	cyclotetramethylenetetranitramine
PETN	Pentaerythritoltetranitrate
TATB	triaminotrinitrobenzene
UF	ultra-fine
DAAF	3,3'-diamino-4,4'-azoxyfurazan

Table Captions

Table 1. Booster formulations, densities, theoretical maximum densities (TMD) and particle sizes.

Shot Number	Booster	Formulation (wt. %)	TMD (g/cc)	Pressed Density (g/cc)	% TMD	Particle Size (μm)
DF8-8807-DE9	Dyed LX-07	90% HMX / 9.95% Viton A / 0.05%Orange Dye	1.896	1.833	96.7	< 300 μm*
DF8-8805-DE9	LX-07	90% HMX / 10% Viton A	1.896	1.835	96.8	< 300 μm*
DF8-8810-DE9	PBX 9504	69.8% micronized TATB / 25% PETN / 5% Kel-F 800 / 0.2% Blue Dye	1.900	1.845	97.1	NA
DF8-8806-DE9	DAAF	Acetonitrile recrystallized, neat-pressed	1.747	1.693	96.9	21 μm **
DF8-8808-DE9	LAX-112 / Kel-F 800	95% LAX-112 / 5% Kel-F 800	1.859	1.733	93.2	~ 20 μm ***
DF8-8809-DE9	LAX-112 / Viton A	90% LAX-112 / 10% Viton A	1.850	1.790	96.8	~ 20 μm ***
DF8-8811-DE9	UF-TATB	Neat-pressed	1.937	1.800	92.9	< 5 μm **

* From sieve specification
** From Coulter particle size analysis
*** From SEM images

Table 2. Summary of experimental results. COI position is referenced to the center of the hemisphere.

Material	FBA (degrees)	Spreading Efficiency	COI (mm)	Excess Transit Time (μs)	Comments
DAAF	70.1	0.78	-11.6	5.2	Large Perturbation
PBX 9504	64.5	0.72	-2.4	7.0	Small Perturbation
Dyed LX-07	63.8	0.71	-15.3	~5.3	Nominal
LX-07	62.8	0.70	-14.4	5.3	Nominal
UF-TATB	16.2	0.18	-3.8	7.2	Hole Punching
LAX-112 / Viton A	---	---	---	---	Failure
LAX-112 / Kel-F 800	---	---	---	---	Failure

Figure Captions

Figure 1. Cutaway of the experimental assembly showing complete charge on the aluminum fixture.

Figure 2. Molecular structures of DAAF and LAX-112.

Figure 3. Scanned film for all successful experiments. Streak records for all are overlaid on the still photo for LX-07. The write speed of the camera was 12 mm/μs, but reproduction in the figure is not actual size.

Figure 4. Digitized and combined records for all successful experiments. Note that the fiducial detonator was missed for the Dyed LX-07 experiment, so the position of breakout time is not accurate.

Figure 5. Geometric construction for constructing the detonation wave shape.

Figure 6. Geometric construction for determining the angle between the emerging detonation wave and the observation ball surface.

Figure 7. Wave reconstruction for all successful experiments. The inner wave reconstruction (blue) is pushed back from first breakout, the outer wave reconstruction (green) is pulled forward from last breakout, and the middle reconstruction (maroon) is the average of the other two. The position of the last breakout varied from shot to shot, having a large affect on the outer wave reconstruction most notably for PBX 9504 and UF-TATB. This difference has a large influence on COI position.

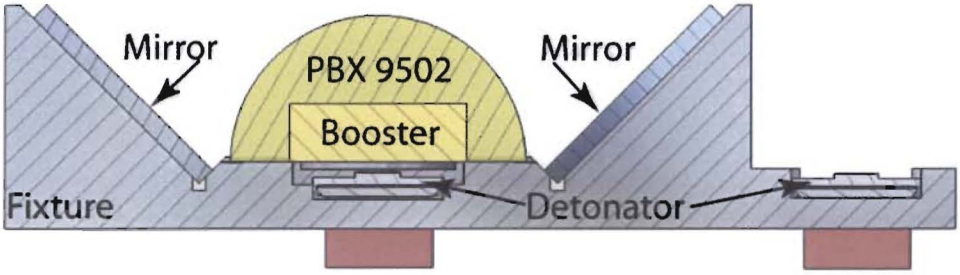

Figure 1

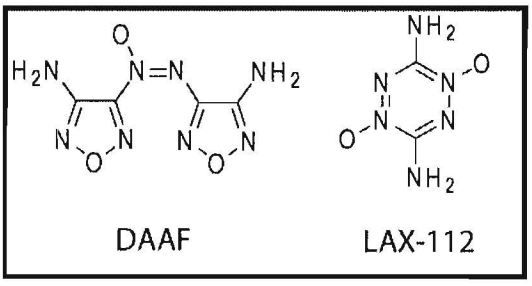

Figure 2

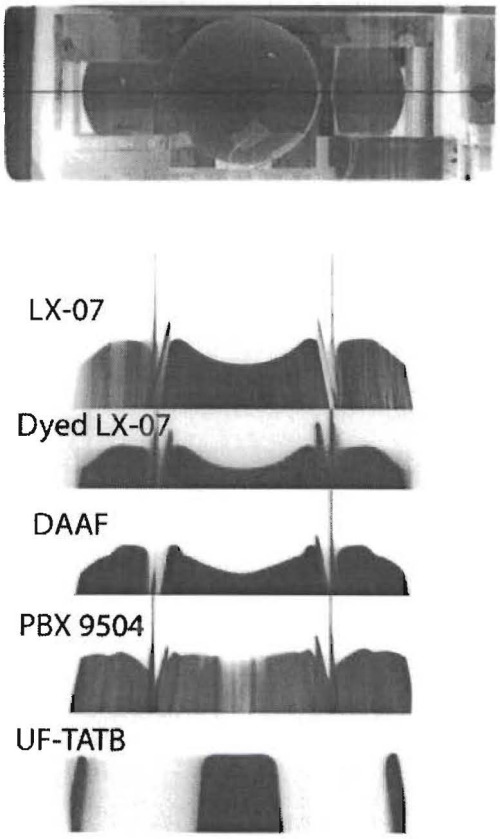

Figure 3

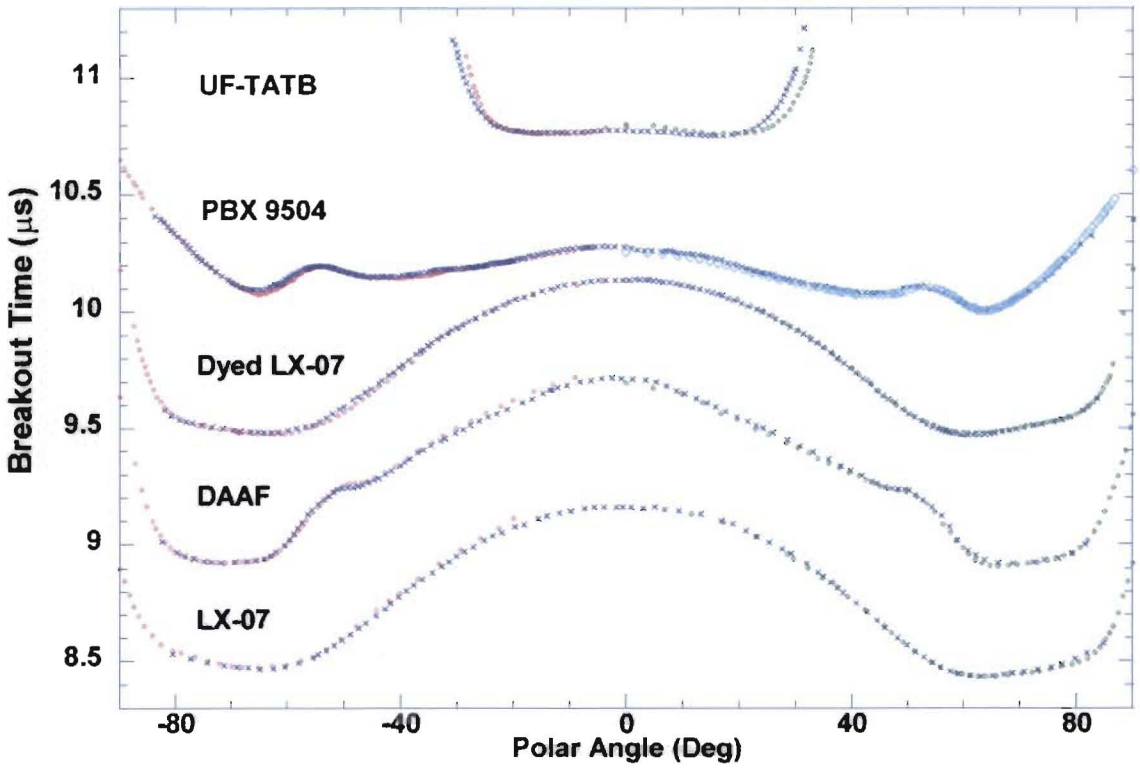
UF-TATB
PBX 9504
Dyed LX-07
DAAF
LX-07
Breakout Time (μs)
11
10.5
10
9.5
9
8.5
-80
-40
0
40
80
Polar Angle (Deg)

Figure 4

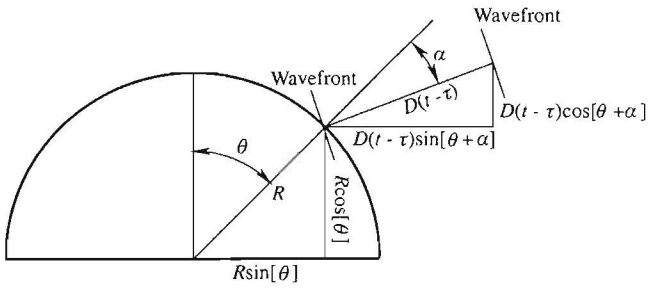
Wavefront
Wavefront
α
D(t - τ)
D(t - τ)cos[θ +α]
D(t - τ)sin[θ +α]
θ
R
Rcos[θ]
Rsin[θ]

Figure 5

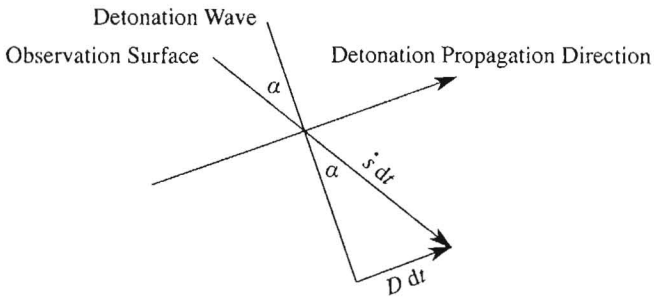
Detonation Wave
Observation Surface
Detonation Propagation Direction
α
α
ṡ dt
D dt

Figure 6.

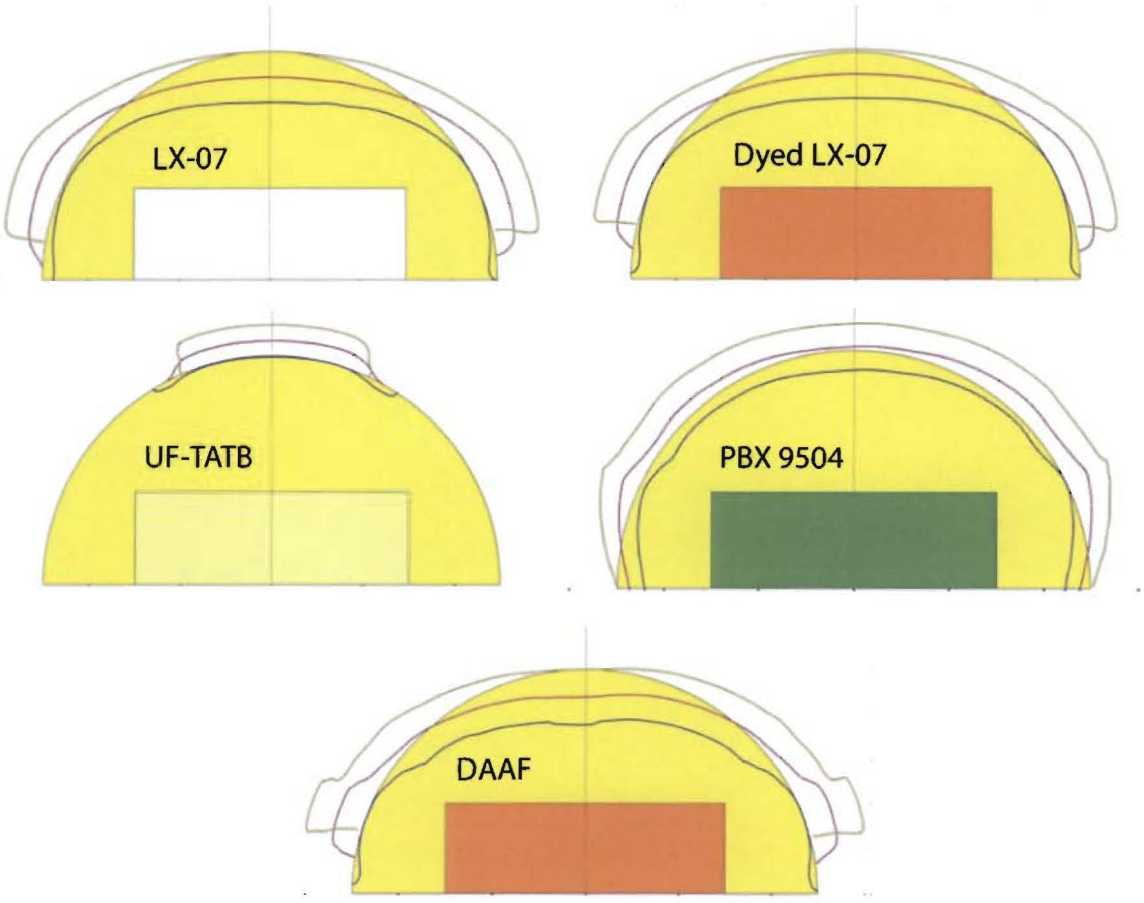

Figure 7